Biotechnology Advances 31 (2013) 362–368

Contents lists available at SciVerse ScienceDirect

Biotechnology Advances

journal homepage: www.elsevier.com/locate/biotechadv

Research review paper

Very small photoluminescent gold nanoparticles for multimodality biomedical imaging☆

Sheng-Feng Lai [a,b], Chia-Chi Chien [b], Wen-Chang Chen [a,**], Hsiang-Hsin Chen [b], Yi-Yun Chen [b], Cheng-Liang Wang [b], Y. Hwu [b,c,d,*], C.S. Yang [e], C.Y. Chen [f], K.S. Liang [g], Cyril Petibois [h], Hui-Ru Tan [i,j], Eng-Soon Tok [i,j], G. Margaritondo [k]

[a] Department of Chemical and Materials Engineering, National Yunlin University of Science and Technology, Yunlin 640, Taiwan
[b] Institute of Physics, Academia Sinica, Nankang, Taipei 115, Taiwan
[c] Department of Engineering and System Science, National Tsing Hua University, Hsinchu 300, Taiwan
[d] Advanced Optoelectronic Technology Center, National Cheng Kung University, Tainan 701, Taiwan
[e] Center for Nanomedicine, National Health Research Institutes, Miaoli 350, Taiwan
[f] National Synchrotron Radiation Research Center, Hsinchu 300, Taiwan
[g] Electrophysics Department, National Chiao Tung University, Hsinchu 300, Taiwan
[h] Université de Bordeaux, CNRS UMR 5248-CBMN, F33405 Talence-Cedex, France
[i] Physics Department, National University of Singapore, Singapore 117542
[j] Institute of Materials Research and Engineering, A*STAR, S117602, Singapore
[k] Ecole Polytechnique Fédérale de Lausanne (EPFL), CH-1015 Lausanne, Switzerland

ARTICLE INFO

Available online 30 May 2012

Keywords:
Photoluminescence
Au nanoparticles
X-ray imaging
Cellular uptake
Radiation synthesis
Cytotoxicity
Tumor development

ABSTRACT

An original synthesis method based on X-ray irradiation produced gold nanoparticles (AuNPs) with two important properties for biomedical research: intense visible photoluminescence and very high accumulation in cancer cells. The nanoparticles, coated with MUA (11-mercaptoundecanoid acid), are very small (1.4 nm diameter); the above two properties are not present for even slightly larger sizes. The small MUA-AuNPs are non-cytotoxic (except for very high concentrations) and do not interfere with cancer cell proliferation. Multimodality imaging using visible light fluorescence and X-ray microscopy is demonstrated by tracing the nanoparticle-loaded tumor cells.

Contents

☆ A new type of Au nanoparticles showing strong photoluminescence and high cellular uptake enables in vivo multimodality (X-ray and visible light) imaging and tracing of mouse tumors.

* Correspondence to: Y. Hwu, Institute of Physics, Academia Sinica, Nankang, Taipei 115, Taiwan. Fax: +886 2 2789 6721.
** Correspondence to: W.-C. Chen, Department of Chemical and Materials Engineering, National Yunlin University of Science and Technology, Yunlin 640, Taiwan.
E-mail addresses: ChenWC@yuntech.edu.tw (W.-C. Chen), phhwu@sinica.edu.tw (Y. Hwu).

0734-9750/$ – see front matter
doi:10.1016/j.biotechadv.2012.05.005

1. Introduction

The interaction of AuNPs with cells was intensively investigated (Besner et al., 2009; Daniel and Astruc 2004; Ghosh et al., 2008; Giljohann et al., 2010; Jana et al., 2001; Sau et al., 2001; Schwartzberg et al., 2004; Sivaraman et al., 2010; Yang et al., 2008), in particular as far as physical and biological size effects are concerned (Alkilany and Murphy 2010; Connor et al., 2005; Murphy et al., 2008; Ryan et al., 2007; Shah et al., 2011; Wang SG et al., 2008). However, the properties of very small (<2 nm) nanoparticles are still only partially known. There is an apparent conflict between two basic requirements for biomedical applications: photoluminescence (e.g., for cancer cell tracing) and strong cell accumulation. Indeed, Zheng et al., and other authors (Bo et al., 2007; Duan and Nie; 2007; Lin et al., 2009 Zheng et al., 2007) reported photoluminescence from very small AuNPs or nanoclusters. In parallel, few reports (Chithrani et al., 2006; Jiang et al., 2008) argued that larger (15–50 nm) AuNPs produce the strongest cell accumulation effects.

We were able to reconcile these two properties by using MUA capping and an original synthesis method based on X-ray irradiation of the precursor solution. This approach produced very small (1.4 nm) MUA-AuNPs that are photoluminescent and strongly accumulate in

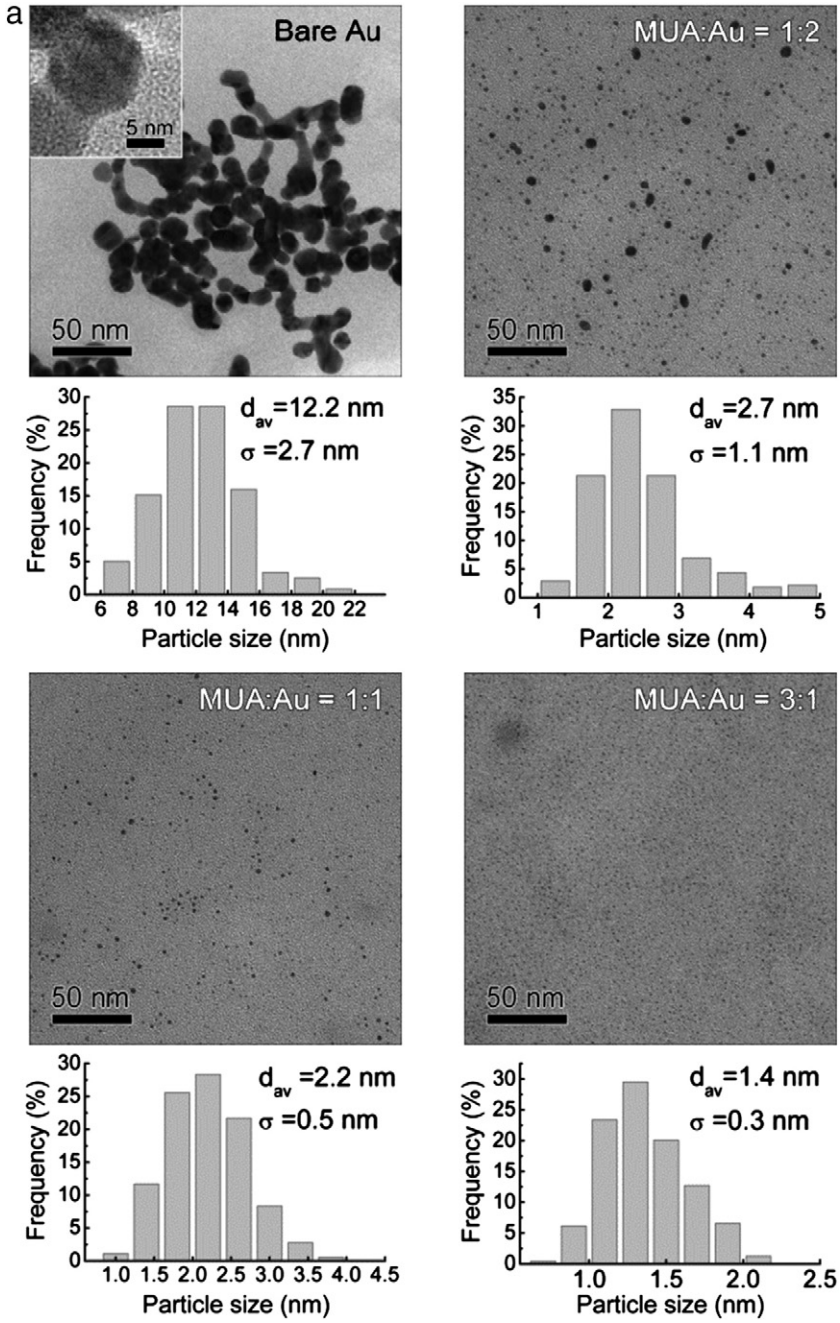

Fig. 1. (a) TEM micrographs with the corresponding size histograms ($n > 200$) and (b) UV–visible spectra of AuNPs synthesized without MUA and with MUA/Au ratios $R = 0.5$, 1 and 3. (c) SAXS scattering profiles of MUA-AuNP colloids with 1 and 0.1 mg ml^{-1} concentration. The 1 mg ml^{-1} profile shows the peaks of interparticle interference at scattering vector magnitudes $q = 0.015$ and 0.034 Å^{-1}, and a hump of the form factor at $q = 0.3$ Å^{-1}. The scattering profile of the 0.1 mg ml^{-1} nanoparticle colloid was fitted using a fuzzy sphere model; the results indicate that the diameter of the nanoparticles plus the MUA coating is ≈3.75 nm.

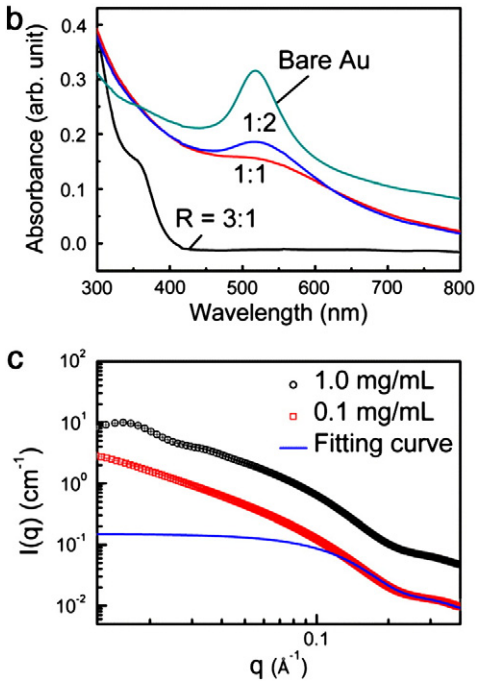

Fig. 1 (*continued*).

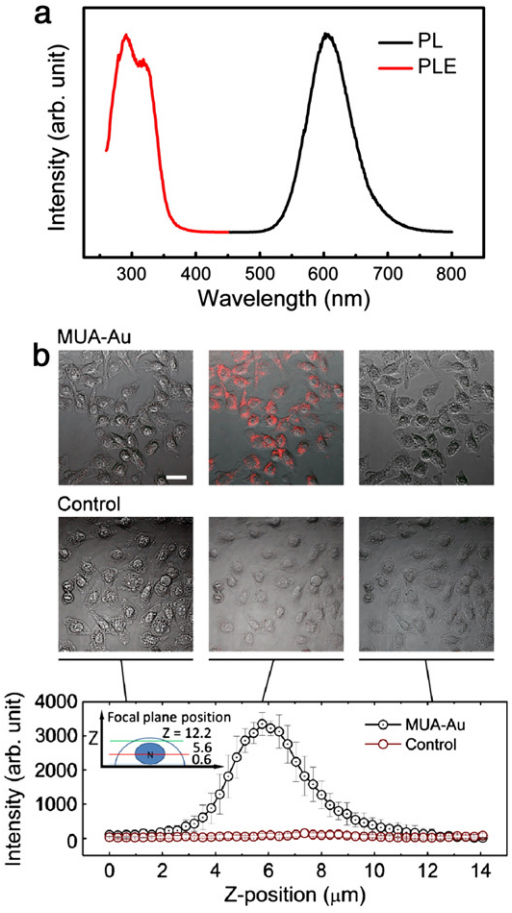

Fig. 2. (a) Photoluminescence (290 nm) and photoluminescence excitation (602 nm) spectra of our 1.4 nm MUA-AuNPs. (b) Confocal photoluminescence microscopy images of EMT-6 cells with 1.4 nm MUA-AuNPs at different *Z*-positions (see inset in the bottom part). The photoluminescence was excited by a 405 nm laser. The control images were obtained without MUA-AuNPs. The curves on the bottom show the integrated photoluminescence intensity (averaged over 10 cells) vs. *Z*.

cancer cells. Furthermore, gold is an X-ray absorber; therefore, our nanoparticles can be also useful for multimodality (photoluminescence and X-ray) imaging.

Both features of the fabrication method – MUA coating and X-ray irradiation – were independently tested in previous studies. X-ray irradiation of the precursor solution produced colloids of metallic nanoparticles and nanorods with very high concentration and excellent long-term stability. (Cai et al., 2010; Liu et al., 2008; Wang et al., 2007a, 2007b, 2008a, 2008b, 2011; Yang et al., 2006) MUA coating was used to control the AuNP dimension down to 1–2 nm, obtain narrow size distributions, and to ensure biocompatibility (Lai et al., 2011). By combining the two features, we discovered that small nanoparticles combine the three interesting properties reported here. The small size is critical for such properties: even a slight diameter increase from 1.4 to 2.2 nm eliminates the photoluminescence and reduces the accumulation in EMT-6 cell by a factor >20.

To analyze these size effects, we irradiated with X-rays precursor solutions with different MUA/Au molar ratios, *R*, that produced different average diameters. Details of the size control and the radiation affect are reported elsewhere (Lai et al., 2012). The nanoparticles were then characterized with a variety of techniques including inductively coupled plasma mass spectrometry (ICP-MS), transmission electron microscopy (TEM), small-angle X-ray scattering (SAXS), Fourier transform infrared (FTIR) spectroscopy, zeta-potential analysis, photoluminescence spectroscopy, cell viability analysis, ultraviolet–visible (UV–VIS) spectroscopy and thermogravimetric analysis (TGA). We report here the results most directly relevant to our main findings.

2. Material and methods

2.1. Materials

$HAuCl_4 \cdot 3H_2O$, MUA, sodium hydroxide, glutaldehyde, and formaldehyde were purchased from Sigma-Aldrich. All chemicals were reagent grade.

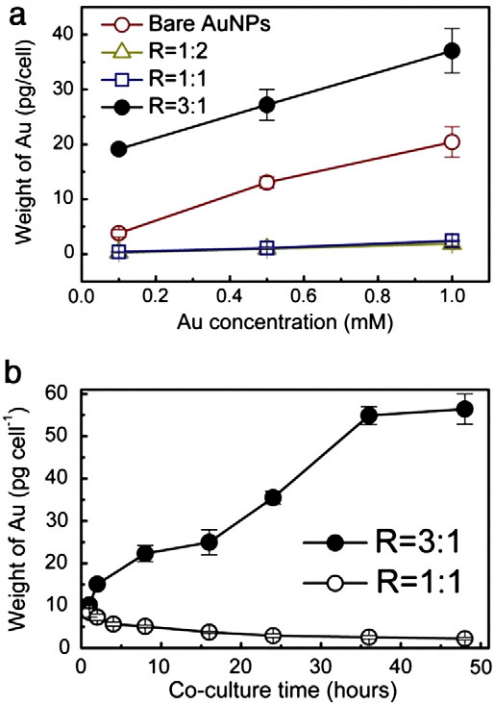

Fig. 3. (a) ICP-MS analysis of MUA-AuNP accumulation in EMT-6 cells as a function of the Au concentration in the solution; the culture time with nanoparticles was 12 hours. (b) ICP-MS analysis of the uptake by EMT-6 cells of MUA-AuNPs ($R = 3$ and 1) vs. the culture time with nanoparticles. 2×10^4 EMT-6 cells were seeded for 36 hours before adding the nanoparticles to the medium.

2.2. Synthesis of MUA-AuNPs

0.5 ml of 20 mM $HAuCl_4 \cdot 3H_2O$ were adjusted to pH ~11 with 0.1 M NaOH. We then added MUA dissolved in anhydrous ethanol with different molar concentrations (relative to Au) and water to reach a 10 ml volume. The solution was placed in polypropylene conical tubes and irradiated for 3 min with hard X-rays from the BL01A beamline of the NSRRC, running at a constant electron current of 300 mA. The X-ray photon energy ranged from 8 to 15 keV and was centered at ~12 keV delivering a dose rate ~4.7×10^5 Gy s^{-1}. (Liu et

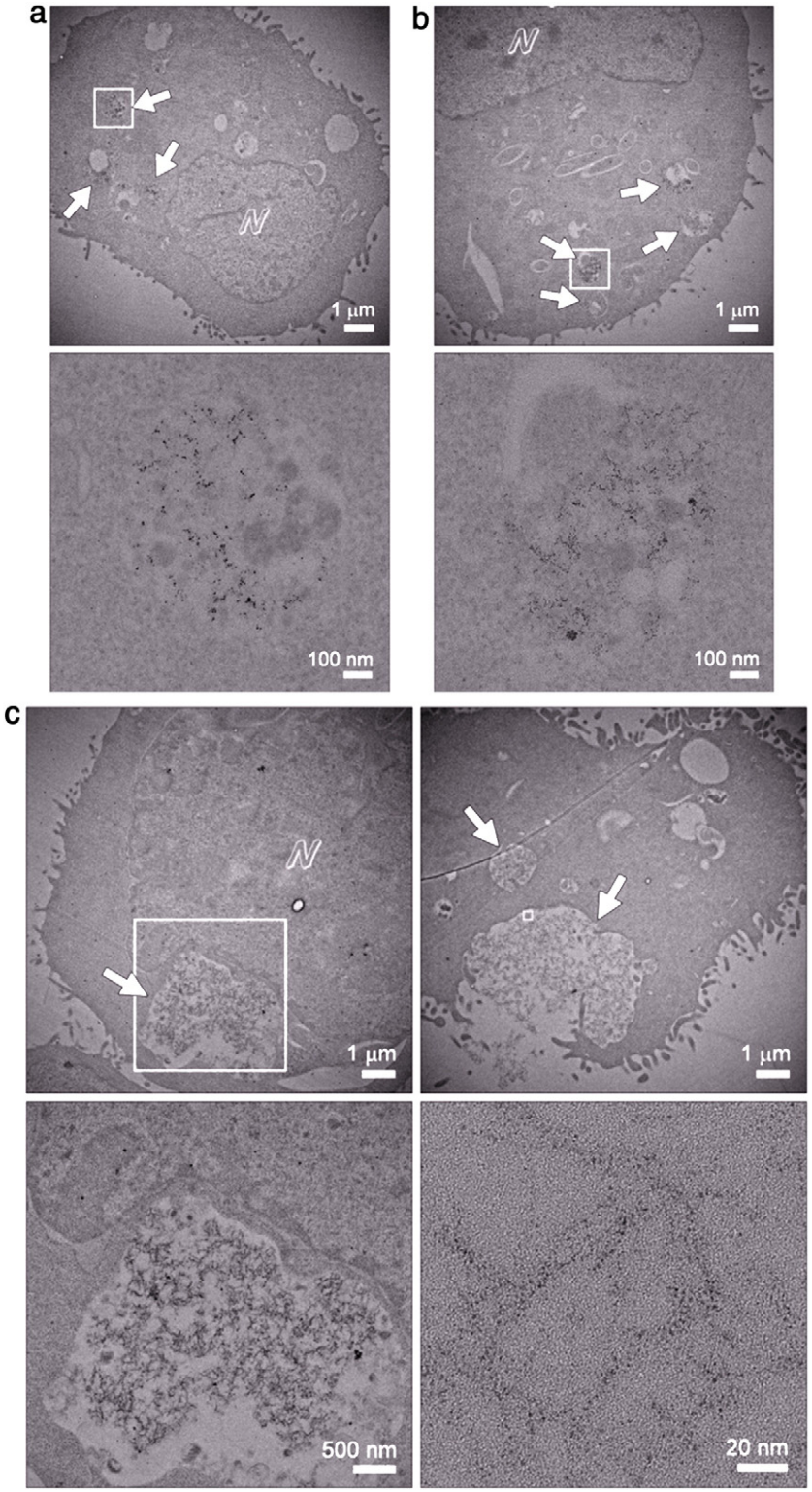

Fig. 4. TEM micrographs of EMT-6 cells cultured for 24 hours with a 0.5 mM Au concentration solution, giving MUA/Au ratio $R = 0.5$ (a), 1 (b), and 3 (c). The bottom images in (a), (b) and (c) correspond to magnified view of the square areas. N is the nucleus.

al., 2009) After the irradiation, the solution was concentrated by centrifugation and the unbound MUA was removed by repeated ultrafiltration with a 10 kDa molecular cutoff.

2.3. Characteristics of the MUA-AuNPs

Samples for TEM were prepared by placing a drop of the solution on a carbon-coated copper grid and dried at 40 °C. TEM measurements were performed in a JEM-2100F system at an accelerating voltage of 200 kV. UV–visible spectra were acquired over 200–800 nm using a USB4000 Fiber Optic spectrometer from Ocean Optics (Dunedin, USA) with 1 cm path length cuvette (Evergreen Scientific, USA). Small angle X-ray scattering measurements were taken at the BL23A beamline of NSRRC with 15 keV photon energy and 1820.88 mm specimen-to-detector (MarsCCD 1024×1024 pixels) distance on 1 mg ml^{-1} and 0.1 mg ml^{-1} of the $R=3$:1 MUA-AuNPs. Photoluminescence spectra were measured at room temperature with a Cary Eclipse spectrophotometer (Varian, USA).

2.4. Quantitative analysis of cellular uptake of MUA-AuNPs

After preparing the EMT-6 cell as described above and waiting overnight, different concentrations of the MUA-AuNPs were added at different times. After culturing with nanoparticles, the cells were trypsinized, counted and exposed to a freshly prepared aqua regia solution in an ultrasonic bath for 3 hours. The Au content of the cells was then measured by ICP-MS with an Agilent 7500cx Instrument.

2.5. Confocal microscopy

After preparing the EMT-6 cell culture and after 32 hours culturing, a 0.1 mM Au concentration equivalent of the MUA-AuNPs with a MUA/Au molar ratio of 3 was added and cultured for 24 hours. Afterwards, the cells were washed three times with 1× PBS, fixed in 4% formaldehyde solution for 10 min and placed in a PBS solution for direct observation by a confocal microscopy (Olympus IX71) with 405 nm laser excitation.

2.6. TEM observations of cell uptake

The cells were cultured on a 10 cm dish at 37 °C in a humidified 5% CO_2 atmosphere. After 24 hours, 0.5 mM of MUA-AuNP solution was added and cultured for 24 hours; the cells were then washed with 1× PBS three times, trypsin treated, fixed in 2% glutaldehyde solution for 1 hour and stained with 1% osmium tetroxide. Then, dehydration was achieved by sequential treatment with 30%, 45%, 60%, 75%, 95% and 100% ethanol, followed by 100% resin infiltration and embedding. Ultrathin sections (100 nm) prepared by an ultramicrotome were finally placed on copper grids.

BALB/c mice (20±2 g, 4 weeks old) were acquired from the National Laboratory Animal Center, fed with sterile food and sterile water with pH, and kept at 7.0–7.5, while housed in isolated cages with a 12-h light/dark cycle. CT-26 cells were cultured with 500 μM MUA-AuNPs in medium RPMI-1640 with 10% FBS (fetal bovine serum) and grown in a 5% CO_2 incubator. After culturing for 24 hours, cells 1×10^6 cells per 100 μl were injected via tail vein for metastatic lung cancer development; 5×10^5 cells per 50 μl were locally injected in for metastatic liver cancer development spleen for 26 days. EMT-6 cells were cultured with 500 μM MUA-AuNPs for 24 hours, after trypsin treatment. Then, harvested cells were added to PBS. Fifty microliters of 1×10^7 cells ml^{-1} EMT-6 cell solution were inoculated in the subcutaneous tissue of the left thigh region.

3. Results and discussion

Fig. 1 illustrates the effects of MUA on the nanoparticle size. Fig. 1(a) compares TEM images (by a JEM-2100F system operating at 200 kV) of bare-AuNP and MUA-AuNP samples prepared by placing a drop of the colloid on a carbon-coated copper grid and drying at 40 °C. The size effects are evident; we derived from images of this type average diameters of 12.2, 2.7, 2.2 and 1.4 nm for bare AuNPs and for MUA-coated AuNPs corresponding to $R=0$, 0.5, 1 and 3; no further size decrease was observed for R-values above 3.

The UV–visible spectra of Fig. 1(b) confirm this progressive size decrease—see the blue shift and gradual suppression of the Au surface plasmon peak. Fig. 1(c) shows SAXS results; by fitting them with the fuzzy sphere model, we confirmed an overall size <4 nm including the MUA coating (Stieger et al., 2004). As R increases, not only the size decreases but also the size distribution width, reaching ±0.27 nm (~±20%) for $R=3$.

Fig. 2 shows that our 1.4 nm MUA-AuNPs do produce photoluminescence, perhaps due to quantum confinement effects (Huang et al., 2007; Zheng et al., 2003). No photoluminescence was observed instead for larger MUA-AuNPs or bare AuNPs. Fig. 2(a) shows the photoluminescence (PL) (black) and photoluminescence excitation (PLE) (red) spectra measured at room temperature with a Varian Cary Eclipse spectrophotometer.

Fig. 2(b) shows confocal visible micrographs under laser excitation (405 nm) of EMT-6 cells after 24 hour culture with 1.4 nm MUA-AuNPs, triple 1× PBS washing, fixing in 4% formaldehyde solution for 10 min and replacement in a 1× PBS solution. The images were taken for different focal positions along the Z-axis, perpendicular to the substrate (see the inset in the bottom part). Note the photoluminescence in the top-middle image.

The bottom part of Fig. 2(b) shows the emitted intensity vs. Z. Basically, the most intense photoluminescence originates from the middle of the cells, apparently from the area surrounding the cell nucleus. This implies of course that the photoluminescent nanoparticles are inside the cell rather than on the membrane. This demonstrates that AuNPs accumulated in cytosol without crossing the nuclear membrane, thus preventing interaction with nucleus. This cytosolic accumulation also suggests that Au-NPs were vesiculated.

Fig. 3 deals with the nanoparticle accumulation in cancer cells. Fig. 3(a) shows the total Au equivalent accumulation in EMT-6 cells for different R-values. The results were obtained with an ICP-MS instrument, after trypsinizing, counting and exposing the cells to a fresh aqua regia solution in an ultrasonic bath for 3 hours. Note the strong accumulation for the smallest nanoparticles (1.4 nm) and

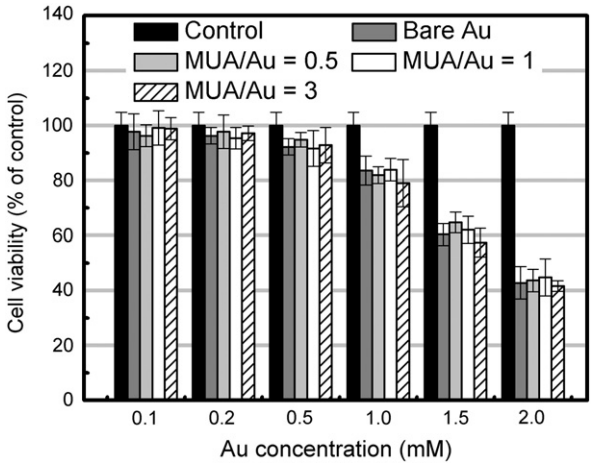

Fig. 5. Cell viability assay of EMT-6 cells co-cultured for 24 hours with different Au concentrations in culture medium and for different R-values.

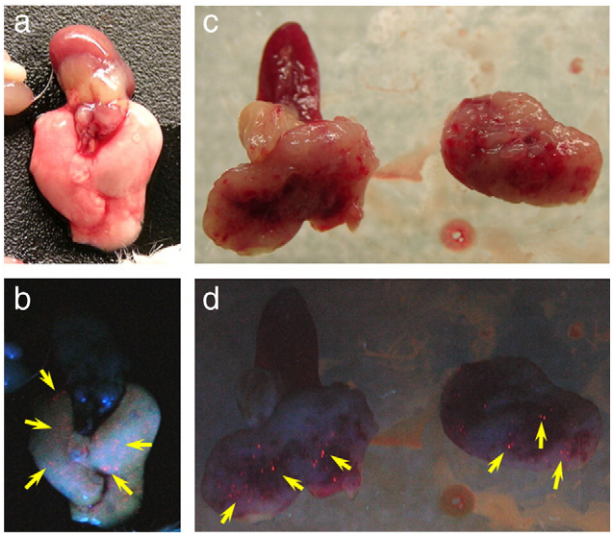

Fig. 6. Photoluminescent MUA-AuNP-loaded CT-26 cells detected in lung (a and b) and spleen tissues (c and d). (a) and (c) are optical images produced by visible light illumination. (b) and (d) are images obtained under exposure to UV light (wavelength: 260 nm): examples of photoluminescent tumor cells are marked by arrows. (c) and (d) show a mouse spleen with a developed a tumor; the organ is cut in two. The dark red portion (top) of the left part is the healthy region showing no photoluminescence. Photoluminescent spots are visible instead in the tumor-containing part of the spleen.

the aforementioned dramatic decrease for slightly larger (2.2 nm) diameters.

These results should be compared to previous reports (Chithrani & Chan, 2007; Chithrani et al., 2009; Jin et al., 2009; Malugin & Ghandehari 2010; Wang et al., 2010; Zhang et al., 2009a) that optimal cell accumulation for AuNPs occurs for 20–50 nm diameters. Our tests for bare nanoparticles are generally consistent with this conclusion. However, we found that MUA-coating drastically changes the situation: the accumulation is best for the smallest nanoparticles.

Fig. 3(b) shows that the accumulation per cell of the 1.4 nm MUA-AuNPs, already high after 12 hours of culture, further increases with the culture time for at least 36 hours. The accumulation per cell for 2.2 nm MUA-AuNPs decreases instead with time: this is due to the fast increase of the cell number by proliferation. The uptake of MUA-AuNPs did not induce detectable effect on cells proliferation, providing further evidence that the nanoparticles are highly biocompatible. Note that the accumulation of 1.4 nm MUA-AuNPs in EMT-6 cells is high not only with respect to larger nanoparticles but also in absolute terms. The level reaches indeed ~57 pg/cell, equivalent to $\sim 2.1 \times 10^9$ nanoparticles/cell and to a total of $\sim 1.0 \times 10^{11}$ available binding sites on MUA per cell (since the average is ~49 for each MUA-AuNP). To the best of our knowledge, such accumulation levels were not reported for this or any other kind of cells which also suggests high biocompatibility.

The above main results were complemented by those of many other tests. The TEM measurements of Fig. 4 show examples of MUA-AuNPs for $R = 0.5$, 1 and 3 in the cell cytoplasm. These nanoparticles were found to be compartmentalized in cytoplasm due to endocytosis. We detected in particular 1.4 nm AuNPs in the high magnification TEM images, Fig. 4(c), indicating an endocytosis internalization route consistent with the fluorescence microscopy results, i.e., with strong accumulation only in the cytoplasm area. These TEM images did not reveal any nanoparticles in the nucleus. These findings confirmed the photoluminescence results: the nanoparticles were primarily present in the cytoplasm area and no nanoparticles were found in the nucleus.

Without involving another internalization route, the very high uptake of the 1.4 nm MUA-AuNPs can only be explained by a similarly high accumulation on the cell surface, which is likely due to a stronger surface interaction related to the special surface properties of the AuNPs. Whether such interaction is due to the higher concentration of MUA molecules or the smaller AuNP size is not clear at present.

We also performed preliminary tests on using our photoluminescent nanoparticles for drug delivery. Specifically, we analyzed MUA as a linker to conjugate doxorubucin and other cancer drugs. The first results show that the conjugation occurs without significantly affecting the MUA-AuNPs photoluminescence.

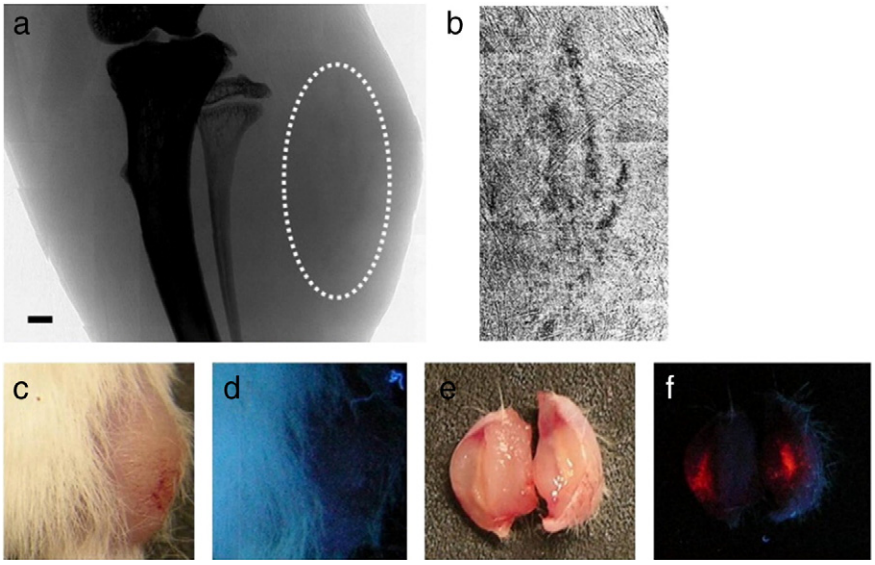

Fig. 7. (a) Projection view of a mouse leg taken in vivo with high resolution microradiography showing a tumor induced by EMT-6 cells loaded with photoluminescent MUA-AuNPs. Scale bar: 500 μm. The dashed ellipse marks the area where the EMT-6 cells were inoculated 6 days before image acquisition. The zoomed-in view (b) emphasizes the cell location by artificial enhancement of the image contrast. The photoluminescence cannot travel through thick tissue and therefore is not visible in picture (d); to detect it, the tissue must be incised as in (e) and (f). Photoluminescence visible at shallow locations underneath the surface (f) indicates that the MUA-AuNPs were transported to the tumor boundary after several generations of cell division. (c) and (e) are photographic images of the tumor at the original subcutaneous location and after incision. (d) and (f) are the corresponding images under photoluminescence-inducing UV illumination.

As far as accumulation in cells is concerned, we explored the possibility that the accumulated nanoparticles are subsequently excreted. However, tests performed by replacing the nanoparticle colloid with DMEM/F12 medium provided no evidence for this hypothesis.

Particularly important are the results on cytotoxicity, obtained by cell trypsination and counting with a hemocytometer. Figs. 5 shows that little or no cytotoxicity up to an equivalent Au concentration of 1.0 mM in the culture medium, whereas the cell viability did decrease beyond 1.0–1.5 mM. This is consistent with other studies (Huang et al., 2007; Li et al., 2009; Naqvi et al., 2010; Zhang et al., 2009b; Zheng et al., 2003). However, our results do not agree with the notion that <1.8 nm gold nanoparticles are highly cytotoxic (Pan et al., 2007). Since the coating molecule is different in previous studies, the observed difference suggests that the surface chemistry of the nanoparticles could play a much more important role in the cell toxicity. In fact, due to the coating our 1.4 nm MUA-AuNPs did not affect cell viability except for the above very high equivalent Au concentrations. The observed acute toxicity in <1.8 nm AuNPs observed by Pan et al. could then be consistent with our finding that is caused by a much higher rate of internalization.

We would like to conclude by mentioning two examples of the possible uses of our photoluminescent nanoparticles. First, we verified that their accumulation makes it possible to easily detect tumors in mice after injecting them from the tail vein (ICP-MS data, not shown). The photoluminescence was still present after the nanoparticles resided in tissue for more than 20 days, with no decrease in intensity.

Second, we found that EMT-6 and CT-26 cells loaded with our photoluminescent nanoparticles kept the ability to develop tumors. As shown in Fig. 6, nanoparticle-loaded CT-26 cells were found in the lung and spleen where their red photoluminescence was clearly visible (yellow arrows in Figs. 6(b) and 4(d)) 10 days after injection from tail veins.

Likewise, MUA-AuNP loaded EMT-6 cells were used to allow tumor growth after subcutaneous inoculation. As shown in Fig. 7, in this case the tumor detection exploited in parallel the photoluminescence for optical imaging and the Au-induced absorption for X-ray imaging. In Fig. 7(a) and (b), the dark features are due indeed to X-ray absorption marking the tumor core.

We can conclude from all these tests that our MUA-AuNPs exhibit, at the same time, very small and uniform size, intense photoluminescence, strong accumulation in cells, high biocompatibility and no interference with cancer cell proliferation. Such characteristics can lead to interesting applications to cancer studies and other domains, some of which were positively tested by preliminary experiments. In particular, the very high surface area to mass ratio, the nearly complete coverage by MUA and the very high cell accumulation makes our nanoparticles good candidates as labeling agents or drug carriers. They are also more likely to be applied for multimodal imaging studies, allowing a comparison of experimental results (by X-Ray imaging, FTIR, Raman, etc.) to conventional photoluminescence and histology analysis for validation.

Acknowledgements

This work was supported by the ANR-NSC French-Taiwan bilateral program no. ANR-09-BLAN-0385, the National Science and Technology Program for Nanoscience and Nanotechnology, the Thematic Research Project of Academia Sinica, the Biomedical Nano-Imaging Core Facility at National Synchrotron Radiation Research Center (Taiwan), the Fonds National Suisse pour la Recherche Scientifique and the Center for Biomedical Imaging (CIBM, supported by the Louis-Jeantet and Leenards foundations).

References

Alkilany AM, Murphy CJ. J Nanopart Res 2010;12:2313.
Besner S, Kabashin AV, Winnik FM, Meunier M. J Phys Chem C 2009;113:9526.
Bo Y, Zhong C, Vu DM, Temirov JP, Dyer RB, Martinez JS. J Phys Chem C 2007;111:12194.
Cai XQ, Wang CL, Chen HH, Chien CC, Lai SF, Chen YY, et al. Nanotechnology 2010;21:335604.
Chithrani BD, Chan WCW. Nano Lett 2007;7:1542.
Chithrani BD, Ghazani AA, Chan WCW. Nano Lett 2006;6:662.
Chithrani BD, Stewart J, Allen C, Jaffray DA. Nanomed Nanotechnol Biol Med 2009;5:118.
Connor EE, Mwamuka J, Gole A, Murphy CJ, Wyatt MD. Small 2005;1:325.
Daniel MC, Astruc D. Chem Rev 2004;104:293.
Duan H, Nie S. J Am Chem Soc 2007;129:2412.
Ghosh P, Han G, De M, Kim CK, Rotello VM. Adv Drug Deliv Rev 2008;60:1307.
Giljohann DA, Seferos DS, Daniel WL, Massich MD, Patel PC, Mirkin CA. Angew Chem Int Ed 2010;49:3280.
Huang CC, Yang Z, Lee KH, Chang HT. Angew Chem Int Ed 2007;119:6948.
Jana NR, Gearheart L, Murphy CJ. Langmuir 2001;17:6782.
Jiang W, Kim BYS, Rutka JT, Chan WCW. Nat Nanotechnol 2008;3:145.
Jin H, Heller DA, Sharma R, Strano MS. ACS Nano 2009;3:149.
Lai SF, Chen WC, Wang CL, Chen HH, Chen ST, Chien CC, et al. Langmuir 2011;27:8424.
Lai SF, Chien CC, Chen WC, Chen YY, Wang CH, Hwu Y, Yang CS, Margaritondo G. RSC Adv 2012;2:6185.
Li JL, Wang L, Liu XY, Zhang ZP, Guo HC, Liu WM, et al. Cancer Lett 2009;274:319.
Lin CAJ, Yang TY, Lee CH, Huang SH, Sperling RA, Zanella M, et al. ACS Nano 2009;3:395.
Liu CJ, Wang CH, Chien CC, Yang TY, Chen ST, Leng WH, et al. Nanotechnology 2008;19:295104.
Liu CJ, Wang CH, Wang CL, Hwu Y, Lin CY, Margaritondo G. J Synchrotron Radiat 2009;16:395.
Malugin A, Ghandehari H. J Appl Toxicol 2010;30:212.
Murphy CJ, Gole AM, Stone JW, Sisco PN, Alkilany AM, Goldsmith EC, et al. Acc Chem Res 2008;41:1721.
Naqvi S, Samim M, Abdin MZ, Ahmed FJ, Maitra AN, Prashant CK, et al. Int J Nanomed 2010;5:983.
Pan Y, Neuss S, Leifert A, Fischler M, Wen F, Simon U, et al. Small 2007;3:1941.
Ryan JA, Overton KW, Speight ME, Oldenburg CM, Loo L, Robarge W, et al. Anal Chem 2007;79:9150.
Sau TK, Pal A, Jana NR, Wang ZL, Pal T. J Nanopart Res 2001;3:257.
Schwartzberg AM, Grant CD, Wolcott A, Talley CE, Huser TR, Bogomolni R, et al. J Phys Chem B 2004;108:19191.
Shah NB, Dong JP, Bischof JC. Mol Pharm 2011;8:176.
Sivaraman SK, Kumar S, Santhanam V. Gold Bull 2010;43:275.
Stieger M, Pedersen JS, Lindner P, Richtering W. Langmuir 2004;20:7283.
Wang CH, Chien CC, Yu YL, Liu CJ, Lee CF, Chen CH, et al. J Synchrotron Radiat 2007a;14:477.
Wang CH, Hua TE, Chien CC, Yu YL, Yang TY, Liu CJ, et al. Mater Chem Phys 2007b;106:323.
Wang CH, Liu CJ, Wang CL, Hua TE, Obliosca JM, Lee KH, et al. J Phys D Appl Phys 2008a;41:195301.
Wang SG, Lu WT, Tovmachenko O, Rai US, Yu HT, Ray PC. Chem Phys Lett 2008b;463:145.
Wang SH, Lee CW, Chiou A, Wei PK. J Nanobiotechnol 2010;8:33.
Wang CL, Hsao BJ, Lai SF, Chen WC, Chen HH, Chen YY, et al. Nanotechnology 2011;22:065605.
Yang YC, Wang CH, Hwu YK, Je JH. Mater Chem Phys 2006;100:72.
Yang Y, Yan Y, Wang W, Li JR. Nanotechnology 2008;19:175603.
Zhang SL, Li J, Lykotrafitis G, Bao G, Suresh S. Adv Mater 2009a;21:419.
Zhang XD, Guo ML, Wu HY, Sun YM, Ding YQ, Feng X, et al. Int J Nanomed 2009b;4:165.
Zheng J, Petty JT, Dickson RM. J Am Chem Soc 2003;125:7780.
Zheng J, Nicovich PR, Dickson RM. Annu Rev Phys Chem 2007;58:409.